# Impulse Response Modeling of Indoor Radio Propagation Channels

Homayoun Hashemi, *Member, IEEE*

*Abstract*—**If indoor radio propagation channels are modeled as linear filters, they can be characterized by reporting the parameters of their equivalent impulse response functions. In this paper, the measurement and modeling of estimates for such functions in two different office buildings are reported. The resulting data base consists of 12 000 impulse response estimates of the channel, which are obtained by inverse Fourier transforming of the channel's transfer functions.**

**Major results of the analysis are as follows. i) The number of multipath components in each impulse response estimate is a normally-distributed random variable with a mean value that increases with increasing antenna separations. ii) A "modified Poisson" distribution shows a good fit to the arrival time of the multipath components. iii) Amplitudes are lognormally distributed over both local and global areas, with a log-mean value that decreases almost linearly with increasing excess delay. iv) For small displacements of the receiving antenna, the amplitude of the multipath components are correlated; the correlation coefficient is a decreasing function of both displacement of the antenna position and excess delay. v) The amplitudes of adjacent multipath components of the same impulse response function show negligible correlations. vi) The rms delay spread over large areas is normally distributed with mean values that increase with increasing antenna separation. The average rms delay spread for each location has great linear dependence with the average path loss for that location. Results reported in this paper can be used in the simulation of indoor radio propagation channels.**

## I. Introduction

An important consideration in successful implementation of personal communication services (PCS) is indoor radio communications, i.e., transmission of voice and data to people on the move inside buildings. Indoor radio communication covers a wide variety of situations ranging from communication with individuals walking in residential or office buildings, supermarkets, or shopping malls, etc. to fixed stations sending messages to robots in motion on assembly lines in factory environments of the future.

Multipath fading seriously degrades the performance of communication systems. Unfortunately, one can do little to eliminate multipath disturbances. However, if the channel is well characterized, the effect of these disturbances can be reduced by proper design of the transmitter and receiver. Detailed characterization of radio propagation is, therefore, a major requirement for successful design of indoor communication systems. Such characterization is particularly useful if it leads to a reliable simulation model.

Measurement and modeling of indoor radio propagation channels has been reported in the literature [1]–[22]. Reference [1] is a comprehensive tutorial-survey coverage of the topic. A review of previous work shows a number of unresolved issues or disagreements. For example, there are reports showing that the rms delay spread of the channel's impulse response depends on the transmitter/receiver antenna separation [11], [20], while no such dependence was observed by other investigators [9], [21]. In one report, the distribution of the arrival times of individual multipath components for wideband data collected in several college buildings was shown to follow a *modified Poisson process* [16]. In another work, impulse response estimates measured in office environments showed that a *double Poisson model* provides a good fit to the empirical data [21]. A third work has shown that neither model provides satisfactory results when applied to propagation data collected at several factory environments [10]. A third example is the statistics of the amplitude of individual multipath components, for which one report shows the distributions to be Rayleigh or lognormal with lognormal showing a better fit [16], while another shows Rayleigh or lognormal with Rayleigh showing a better fit [21]. Although some of these differences may be due to differences in the conditions governing the measurements, others may be due to the insufficiency of data. There are also a number of important issues that have received insufficient attention in the literature. A notable example is the correlation between the amplitude of multipath components with the same delay for impulse response estimates of adjacent components of the same profile. With one exception (the work reported in [10]), no quantitative results have been reported.

During a recent measurement campaign, an extensive multipath propagation data base was set up. The purposes of these measurements were to characterize indoor radio propagation channels, to resolve some of the previously mentioned issues, and to obtain a statistical model of the channel that renders itself properly to later computer simulation. The data base includes 12 000 impulse response functions collected in two office buildings. The measurement plan and the results of statistical modeling are reported in this paper.

## II. Mathematical Model

Random and complicated indoor radio propagation channels can be characterized using the impulse response approach: at each point in a three-dimensional environment, the channel

Manuscript received March 1992; revised December 1992. This work was presented at the 42nd Annual IEEE Vehicular Technology Society Conference, Denver, CO, May 11–13, 1992. This work was performed during the author's sabbatical leave at NovAtel Communications Ltd., Calgary, Canada.

The author is with the Department of Electrical Engineering, Sharif University of Technology, Teheran, Iran.

IEEE Log Number 9210916.

is modeled as a linear filter with a complex-valued lowpass equivalent impulse response which can be expressed as

$$h(t) = \sum_{k=0}^{N-1} a_k \delta(t - t_k) e^{j\theta_k} \quad (1)$$

where $N$ is the number of multipath components; $\{a_k\}$, $\{t_k\}$, $\{\theta_k\}$ are the random amplitude, propagation delay, and phase sequences, respectively; and $\delta$ is the Dirac delta function. Static channels are completely characterized by these path variables.

The previous model was first suggested by Turin [23] to describe multipath fading channels. It provided a consistent model for characterizing [24], [25] and simulating [26] the urban (mobile) radio channel. The mathematical model of (1) and the subsequent simulation model [also based on (1)] have been used as effective tools in the performance analysis of various communication systems operating in the urban multipath channel (see, e.g., [27] and [28]).

It is important to note that this is a wideband model which has the advantage that, because of its generality, it can be used to obtain the response $y(t)$ of the channel to the transmission of *any* signal $s(t)$ by convolving $s(t)$ with $h(t)$ and adding noise

$$y(t) = \int_{-\infty}^{\infty} s(\tau) h(t - \tau)\, d\tau + n(t) \quad (2)$$

where $n(t)$ is the lowpass, complex-value additive Gaussian noise. It should be noted that, due to the motion of people and equipment, the indoor radio propagation channel is, in general, time varying. Therefore, there are two types of variations in the channel: i) variation due to motions in the proximity of the portable unit; and ii) variation due to changes in the static environment. Although i) may have a greater influence than ii), the two are different and, therefore, the characterization described in this paper is applicable only to ii). Temporal variations of the channel have been reported in [19].

## III. Measurement Procedure

### A. Measurement Plan

Since the ultimate goal of the measurement and modeling reported in this paper is to produce a reliable channel simulator, a real-life situation was considered: a portable unit moving in steps through the medium records the channel's impulse response at spatially separated locations. There are three types of variations in the channel's statistics, as depicted in Fig. 1.

*1) Small-Scale Variations:* A number of impulse response profiles collected in the same "local area" are grossly similar since the channel's structure does not change appreciably over short distances. Therefore, impulse responses in the same site exhibit only variations in fine details.

*2) Mid-Scale Variations:* These are variations in the statistics for local areas with the same antenna separation (Fig. 1). As an example, two sets of data collected inside a room and in a hallway, both having the same transmitter/receiver antenna separation, may exhibit great differences. One obvious difference is the total received power at two locations with the same antenna separation. Also, amplitudes at a fixed delay for impulse response estimates collected at two locations with the same transmitter/receiver antenna separation may be very different due to different attenuations in the respective paths.

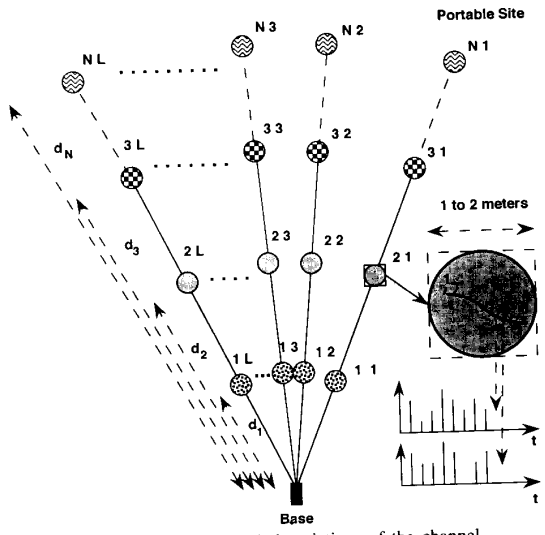


Fig. 1. Local and global variations of the channel.

*3) Large-Scale Variations:* The channel's structure may change drastically when the base-portable distance increases due, among other reasons, to an increase in the number of intervening obstacles. It has been shown by a number of investigators (e.g., [17]) that increasing the antenna separation results in an increase in the large-scale path losses.

The spatially-dependent statistics of indoor channels are different in "local" and "global" areas. Local statistics refer to the small-scale variations described in 1). Global statistics are defined as those when variation type 2) is taken into account. To investigate both local and global statistics, therefore, a measurement plan was devised based on the model of Fig. 1 with $N = 4$, $L = 20$, $J = 75$, $d_1 = 5$ m, $d_2 = 10$ m, $d_3 = 20$ m, and $d_4 = 30$ m. Under this scheme, for each of the two buildings, four antenna separations were considered, twenty 1.5 meter locations were selected per antenna separation, and 75 frequency response estimates with spatial displacements of 2 cm were collected at each area.

Each set of local data is comprised of 75 frequency response estimates collected at one 1.5 m location. Each set of global data consists of 1500 estimates collected at twenty locations with the same antenna separation.

### B. Measurement Sites

The measurement plan was executed at two dissimilar office buildings. Since the geometry of the buildings made it impossible to pick 20 portable locations per fixed site (base), the base sites were also varied for each antenna separation. This procedure brings the added advantage of making the results more general, as compared to a scenario in which a single base location is selected for all measurements.

Building 1 was the NovAtel Communications Ltd. Corporate office located in Calgary, Alberta, Canada. This is a

T-shaped modern three-story facility containing hard partitioned offices, hallways, and laboratory space in addition to a number of soft-partitioned cubicles. Measurements were performed on the first and third floors, with both transmit and receive antennas located on the same floor. The construction of this building is as follows: Inner walls are 406 mm metal stud spacing, with 13 mm gypsum covering. Outer walls are 254 mm concrete slab, with windows from 1.1 to 2.5 m in height. Floors are 254 mm carpeted concrete slab. The ceiling is a suspended type with standard fire-retardant material. Furnishings are standard office furniture and laboratory equipment.

Building 2 was the Alberta Government Telephone Limited (AGT) Tower, also located in Calgary. This is an octagon-shaped building with 27 floors. Measurements were carried out with both transmit and receive antennas on the 19th floor only. The floor plan consists mainly of hard-partitioned hallways and soft-partitioned cubicles with standard office furniture. The construction of this building is as follows: Inner walls are 406 mm metal stud spacing, with 13 mm gypsum covering. Outer walls are 305 mm concrete slab, with 80 mm false wall and heating ducts on the interior. There are windows around the perimeter from 0.8 to 2.4 m in height. Floors are 305 mm carpeted concrete slab. The ceiling is a suspended type with standard fire-retardant material.

The transmitter and receiver sites in each building were chosen carefully to be representative of typical base and portable locations in indoor wireless communication systems. Both line-of-sight (LOS) locations and non-line-of-sight (NLOS) locations (obstructed path between transmitter and receiver) were included. More NLOS locations were selected for larger antenna separations.

In selecting transmit and receive antenna positions at both buildings, care was taken to avoid multipath from structures external to the buildings. This is reflected in the propagation delays of multipath components.

The Bldg 1 data were collected with either one or both of transmit and receive antennas located in laboratories, cubicles, offices, hallways, a lobby, a library, etc. Bldg 2 data, on the other hand, were collected in the more uniform environment of the office space on a single floor. Greater variations (less uniformity) in the environment of Bldg 1 (as compared to Bldg 2) are well reflected in the standard deviations associated with measured parameters.

### C. Measurement Technique

The measurements were performed using a vector network analyzer to measure the frequency response of the indoor propagation channel between two discone antennas. The idea of measuring the frequency response of indoor channels is relatively new [17], [22]. In this method, the channel is excited with tones over a wide range of frequencies. The attenuation and phase shift of each frequency component (caused by the propagation medium) is measured.

The network analyzer swept-frequency band for the measurements reported in this paper was 900 to 1300 MHz in 500 KHz steps (801 points). The time required was 400 ms per sweep, with 10 sweeps being averaged per measurement, making the actual time for each measurement 4 seconds. All measurements were performed at night or on weekends when there were few, if any, other personnel in the vicinity of the measurement setup.

The measured frequency response data were windowed by a minimum three-term Blackman–Harris window [29]. The windowed frequency domain data were then zero padded to the next highest number of points, which is a power of two (1024 for these data). The zeros were padded at either end of the spectrum and the frequency domain data were converted to time domain by IFFT [30].[1]

The frequency step size of 500 KHz results in a maximum measurable time domain delay window of 2 $\mu$s. Windowing in frequency domain is equivalent to interpolation in time domain. The resolution of the impulse response functions is reciprocal of the bandwidth swept (2.5 ns) multiplied by the additional width of the window; actual resolution of 5 ns in the time domain data was, therefore, obtained.

A complete description of the measurement procedure, providing detailed information about each measurement location, the hardware used during measurements, techniques used in the processing of data, etc. is reported in [31]. Sequences of spatially adjacent profiles for line-of-sight and non-line-of-sight paths (antenna separation of 5 m) are reproduced in Fig. 2.

### D. The Discrete-Time Impulse Response Model

A convenient model for characterization of multipath propagation channels is the discrete-time impulse response model [16], [25], [26]. In this model, the time axis is divided into small time intervals called "bins." Each bin is assumed to contain either one multipath component or no multipath component. The possibility of more than one path in a bin is excluded. A reasonable bin size is the resolution of the specific measurement, since two paths arriving within a bin cannot be resolved as distinct paths. Using this model, each impulse response can be described by a sequence of "0"s and "1"s (the path indicator sequence), where a "1" indicates the presence of a path in a given bin and a "0" represents the absence of a path in that bin. To each "1," an amplitude and a phase value are associated. All the data were reduced accordingly using a bin size of 5 ns (resolution of the measurements). Each impulse response function contains 100 bins corresponding to an excess delay of 500 ns. The probability of receiving longer-delayed components was found to be negligible. It is important to note that since absolute timing information is essential for a number of applications [e.g., when calculating the received signal using the convolution integral of (2)], excess delay is measured relative to the delay of the direct path between the transmitter and receiver (16.7, 33.3, 66.7, and 100 ns for antenna separations of 5, 10, 20, and 30 meters, respectively). The first arriving component will, therefore, have an excess delay greater than 0 if it does not arrive over

[1] Measurements at NovAtel were carried out by D. Tholl of TRLabs, who handled all hardware-related problems, selected measurement sites, and processed the frequency domain data to obtain the time-domain data base. Measurements at AGT were carried out by G. Morrison, also of TRLabs.

TABLE I
MEAN ($\mu$) AND STANDARD DEVIATION ($\sigma$) FOR THE NUMBER OF MULTIPATH COMPONENTS $N$ FOR BOTH BUILDINGS, ANTENNA SEPARATIONS OF 5, 10, 20, 30 m, AND $\alpha$ = 10, 20, AND 30 dB

| | Building 1 | | | | | | | | Building 2 | | | | | | | |
|---|---|---|---|---|---|---|---|---|---|---|---|---|---|---|---|---|
| | Antenna Separations (meters) | | | | | | | | Antenna Separations (meters) | | | | | | | |
| | 5 | | 10 | | 20 | | 30 | | 5 | | 10 | | 20 | | 30 | |
| $\alpha$ | $\mu$ | $\sigma$ | $\mu$ | $\sigma$ | $\mu$ | $\sigma$ | $\mu$ | $\sigma$ | $\mu$ | $\sigma$ | $\mu$ | $\sigma$ | $\mu$ | $\sigma$ | $\mu$ | $\sigma$ |
| 10 dB | 3 | 2 | 4 | 2 | 7 | 3 | 8 | 3 | 4 | 2 | 5 | 2 | 5 | 2 | 6 | 3 |
| 20 dB | 8 | 3 | 10 | 3 | 13 | 4 | 17 | 5 | 8 | 3 | 10 | 3 | 11 | 3 | 13 | 4 |
| 30 dB | 13 | 3 | 16 | 3 | 20 | 5 | 24 | 7 | 13 | 3 | 15 | 3 | 18 | 4 | 19 | 4 |

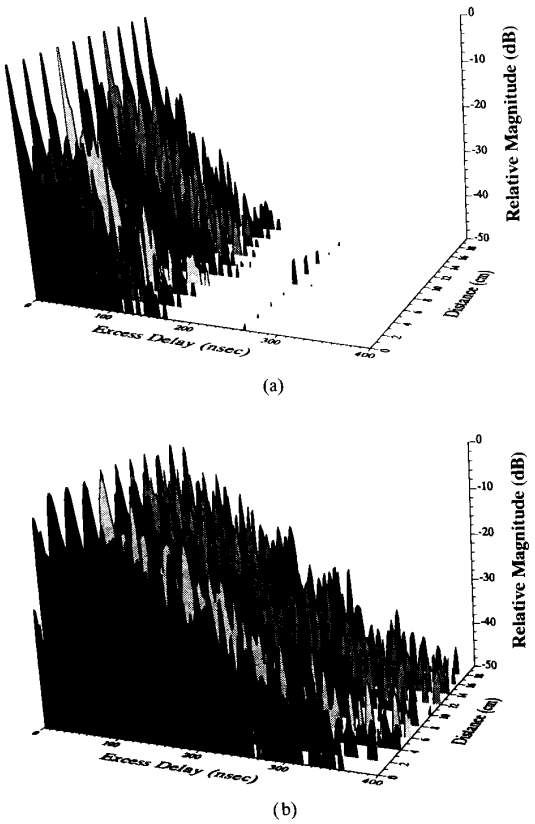


Fig. 2. Sequences of spatially adjacent impulse response functions for Bldg 1, antenna separation of 5 m. (a) A line-of-sight location. (b) A non-line-of-sight location.

the direct path. As a result, bin 0 corresponding to an excess delay of 0 may contain either a "0" or a "1." A component arriving over the direct path (occupying bin 0) may be a strong LOS component, or a component severely attenuated by the intervening structure.

## IV. RESULTS OF THE ANALYSIS

The data collected during the measurements were analyzed with the purpose of characterizing the channel's impulse response, i.e., to determine the statistical properties of the path variables $\{a_k\}$, $\{t_k\}$, and $\{\theta_k\}$. The mathematical model of (1) was, therefore, employed throughout the analysis. Results are described in this section.[2]

### A. Distribution of N

The number of multipath components $N$ for each one of the 6000 profiles collected in each building was calculated. For each profile, $N$ was found by counting all multipath components that were within $\alpha$ dB of the strongest path for $\alpha$ = 10, 20, and 30. The binned data (discrete-time model) were used. The mean and standard deviation of $N$ for each building, each value of $\alpha$, and each antenna separation are summarized in Table I. An examination of this table shows that:

i) There is a clear dependence between the mean value of $N$ and the antenna separation.

ii) The mean value of $N$ increases with increasing $\alpha$. This is expected since, when $\alpha$ increases, more components are included in the calculation of $N$.

iii) Standard deviations increase with increasing the antenna separation. This is due to the fact that there are greater variations in the environment between the transmitter and receiver for larger antenna separations. Also, standard deviations are slightly smaller for most cases of Bldg 2 as compared to Bldg 1. This is reasonable since, as described before, there are fewer variations in the measurement environment of Bldg 2.

[2]D. Lee and D. Ehman of NovAtel Communications Ltd. were responsible for software assistance in processing and analyzing the enormous amount of data collected throughout this project.

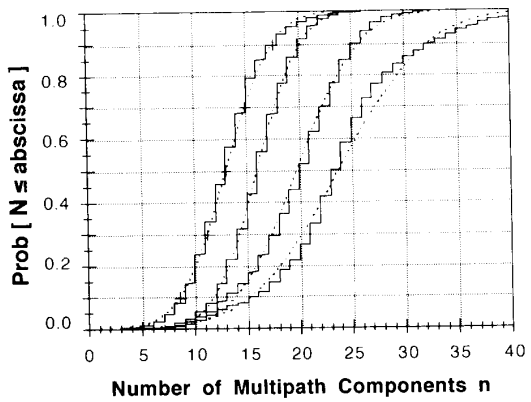


Fig. 3. Distributions of $N$ for Bldg 1. Each set of curves from left to right represent distributions for antenna separations of 5, 10, 20, and 30 m, respectively. Solid curves are empirical distributions and dotted curves are normal fits to the data.

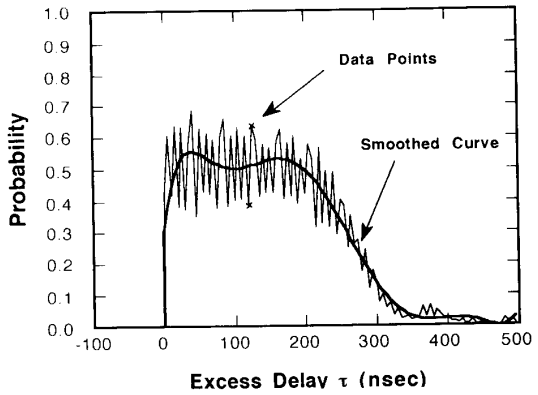


Fig. 4. Probability-of-occupancy curve for Bldg 2, antenna separation of 10 m. The value at a point $\tau$ is the probability of having one multipath component in the interval $(\tau - 2.5,\ \tau + 2.5)$ ns.

The probability distribution of $N$ for Bldg 1, $\alpha = 30$ dB, and for each antenna separation is reproduced in Fig. 3.[3] A normal (or Gaussian) fit to the data is also shown. Each distribution represents 1500 profiles collected at one antenna separation (= 20 locations × 75 profiles per location). Analysis of this plot and others not reproduced shows that, to a very good approximation, $N$ follows a normal distribution. Standard deviations are tabulated in Table I. Observations i) and iii) are also evident in Fig. 3.

The probability of occupancy (i.e., probability of having a multipath component at a fixed delay) for impulse response estimates in Bldg 2, antenna separation of 10 meters, is shown in Fig. 4. All multipath components within 30 dB of the maximum have been included. An inspection of this figure, as well as those not reproduced here, shows that the probability of having a multipath component with an excess delay greater than 400 ns is negligible in the buildings where measurements were made. Given that there were not surrounding buildings, it is accurate to say that the collected data reflect multipath propagation entirely internal to the measured buildings.

### *B. Distribution of the Arrival Time Sequence*

As a preliminary model, one can postulate that the sequence of path arrival times $\{t_k - t_0\}_1^\infty$ follow a Poisson distribution. This distribution is encountered in practice when certain "events" occur with complete randomness (e.g., initiation of phone calls or occurrence of automobile accidents). If $L$ denotes the number of paths occurring in a given interval of time duration $T$, the Poisson distribution requires

$$\text{Prob}(L = \ell) = \frac{\mu^\ell e^{-\mu}}{\ell!} \tag{3}$$

where $\mu = \int_T \lambda(t)\,dt$ is the Poisson parameter. ($\lambda(t)$ is the mean arrival rate at time $t$.) For a stationary process [constant $\lambda(t)$], $E[L] = \text{Var}[L] = \lambda$.

[3]To save space, for each aspect of the analysis only figures for one building are reproduced. Similar results apply to the other building. Exceptions are noted in the text.

Analysis of the measurement data for both buildings and for all antenna separations has established the inadequacy of the Poisson hypothesis to describe the arrival times. Considerable discrepancy was found between the empirical and Poisson fit distributions in every case. The inadequacy of the Poisson distribution is probably due to the fact that scatterers inside a building causing the multipath dispersion are not located with complete randomness. The pattern in location of these scatterers results in deviations from the standard Poisson distribution, which is a purely random event model.

A second-order model that was suggested by Turin *et al.* [24] and developed by Suzuki [25] to describe the path arrival times of the mobile channel is a modified Poisson process (the so-called $\Delta$-$K$ model). It takes into account the clustering property of paths caused by the grouping property of scatterers. This process is described by transitions between two states representing different mean arrival rates. Initially, the process starts in State 1 with a mean arrival rate $\lambda_0(t)$. If a path arrives at time $t$, a transition is made to State 2 with a mean arrival rate $K\lambda_0(t)$. If no further paths arrive in the interval $[t, t + \Delta)$, a transition is made back to State 1 at the end of the interval. For $K = 1$ or $\Delta = 0$, this process reverts to a standard Poisson process. For $K > 1$, the incidence of a path at time $t$ increases the probability of receiving another path in the interval $[t, t + \Delta)$, i.e., the process exhibits a clustering property. For $K < 1$, the incidence of a path decreases the probability of receiving another path, i.e., paths tend to arrive rather more evenly spaced as compared to a standard Poisson model.

The discrete-time version of the previous model has shown a good fit to the empirical data collected in several urban mobile environments [25]. It has also been used in the simulation of the mobile channel [26]. In the discrete-time model, the probability of having a multipath component in bin $i$, $P_i$ is equal to $\lambda_i$ if there was no path in the $(i-1)$st bin and $K\lambda_i$ if there was a path in the $(i-1)$st bin. The "underlying" probabilities of path occurrences $\lambda_i$ can be obtained from the empirical probability of path occurrences (probability

TABLE II
OPTIMUM VALUES OF $K$ AND THE ASSOCIATED MEAN SQUARE ERROR ($e$) FOR SELECTED PORTIONS OF THE EXCESS DELAY AXIS, FOR BOTH BUILDINGS, AND FOR ANTENNA SEPARATIONS OF 5, 10, 20, AND 30 m

| | Building 1 | | | | | | | | Building 2 | | | | | | | |
|---|---|---|---|---|---|---|---|---|---|---|---|---|---|---|---|---|
| | Antenna Separations (meters) | | | | | | | | Antenna Separations (meters) | | | | | | | |
| Excess Delay | 5 | | 10 | | 20 | | 30 | | 5 | | 10 | | 20 | | 30 | |
| Interval (nsec.) | K | e | K | e | K | e | K | e | K | e | K | e | K | e | K | e |
| [0,25) | 1.07 | 0.052 | 0.76 | 0.107 | 0.82 | 0.111 | 0.56 | 0.101 | 0.95 | 0.041 | 0.56 | 0.082 | 0.89 | 0.105 | 1.08 | 0.120 |
| [0,50) | 0.75 | 0.031 | 0.61 | 0.045 | 0.59 | 0,046 | 0.75 | 0.035 | 0.57 | 0.030 | 0.58 | 0.042 | 0.66 | 0.042 | 1.03 | 0.027 |
| [0,75) | 0.57 | 0.023 | 0.52 | 0.027 | 0.51 | 0.026 | 0.70 | 0.019 | 0.46 | 0.027 | 0.58 | 0.021 | 0.56 | 0.021 | 0.79 | 0.019 |
| [0,100) | 0.50 | 0.014 | 0.50 | 0.020 | 0.48 | 0.018 | 0.60 | 0.014 | 0.40 | 0.016 | 0.51 | 0.015 | 0.52 | 0.016 | 0.74 | 0.013 |
| [0,125) | 0.47 | 0.011 | 0.45 | 0.014 | 0.46 | 0.015 | 0.56 | 0.012 | 0.45 | 0.010 | 0.48 | 0.013 | 0.52 | 0.011 | 0.66 | 0.008 |
| [0,150) | 0.47 | 0.009 | 0.44 | 0.011 | 0.46 | 0.012 | 0.57 | 0.011 | 0.42 | 0.009 | 0.47 | 0.009 | 0.52 | 0.009 | 0.64 | 0.007 |
| [0,225) | 0.51 | 0.008 | 0.50 | 0.006 | 0.82 | 0.010 | 1.01 | 0.006 | 0.44 | 0.006 | 0.56 | 0.005 | 0.49 | 0.006 | 0.63 | 0.003 |
| [0,300) | 0.81 | 0.007 | 1.31 | 0.003 | 1.29 | 0.003 | 2.62 | 0.002 | 0.92 | 0.001 | 1.35 | 0.005 | 0.51 | 0.002 | 0.76 | 0.002 |

of occupancy curves—Fig. 4). Mathematical details of this model are described in [25], [26].

Application of this model to the data collected in this project provided consistently good fits between the empirical and theoretical $\Delta$-$K$ model. In the analysis, $\Delta$ was fixed at 5 ns (size of a bin) and optimum $K$ values were obtained using an optimization technique that minimized the mean square error between the experimental and theoretical ($\Delta$-$K$ model) path number distributions. Optimum values of $K$ and the associated mean square error between theoretical and empirical distributions for selected portions of the excess delay axis are shown in Table II. In this table, all multipath components in the excess delay interval $[0, \tau)$ for $\tau$ = 25, 50, 75, 100, 125, 150, 225, and 300 ns were used to calculate the distributions. It is important to note that the optimization process was repeated for each excess delay interval. Fig. 5 represents path number distributions for 1500 arrival-time sequences for Bldg 1 and an antenna separation of 10 m. In this figure, the empirical, Poisson fit, and modified Poisson fit distributions are shown. The vertical axis in Fig. 5 is the probability of having $n$ components in the interval $[0, \tau)$, for $\tau$ = 25, 50, 100, 150, 225, and 300 ns. Similar results were obtained for both buildings, all antenna separations, and for the cases where all 6000 sequences for the same building were combined. Although for ease of presentation the distributions are drawn as curves, they have meaning only at integer values.

Results of this aspect of the analysis are consistent with those obtained in another work [16], although the latter is based on limited data.

The reported goodness of fit of the $\Delta$-$K$ model is due to one or both of two facts.

i) Nonrandomness of the local structure. Entreis in Table II show that for most cases $K < 1$, which indicates that scatterers are more evenly distributed (less clustered) than what the Poisson hypothesis dictates. It is important to note that the resolution of the data is 5 ns. Two multipath components arriving within this time interval (bin), therefore, cannot be resolved as distinct components. As a result, individual contributions from small objects, which may very well be grouped or clustered in space (such as pieces of furniture), are not necessarily represented as distinct multipath contributions in the data.

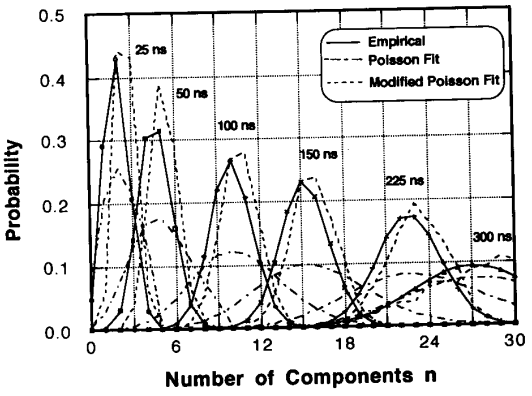


Fig. 5. Empirical, Poisson, and modified Poisson fit to the arrival time sequence for Bldg 1, antenna separation of 10 m.

ii) The $\Delta$-$K$ model uses empirical probabilities associated with individual small intervals of length $\Delta$, while the standard Poisson model uses the total probability associated with a much larger interval $T$ (normally, $T >> \Delta$). Therefore, the $\Delta$-$K$ model uses more information from the data as compared to the standard Poisson model, resulting in better fits between theoretical and empirical distributions.

### C. Statistics of the Amplitude Sequence

*1) Global distributions:* The average value of amplitudes versus excess delay was obtained for each antenna separation. The results for Bldg 2 are reproduced in Fig. 6. Mean amplitudes in these plots are normalized (dB, relative to the peak amplitude of each profile). The nonzero values of curves at 0 excess delay are due to the fact that, in a number of profiles, the

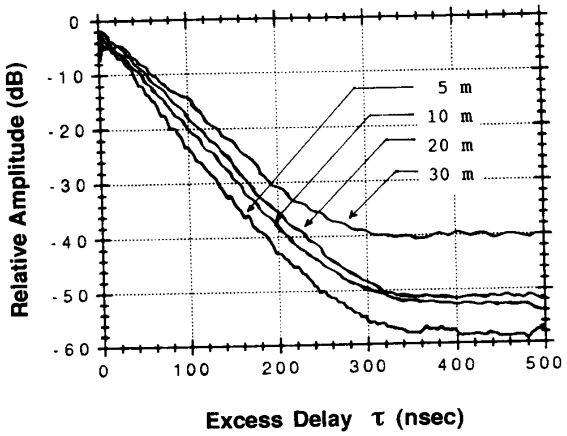


Fig. 6. Mean amplitudes (in dB, relative to the peak amplitude of each profile) versus excess delay for all antenna separations of Bldg 2.

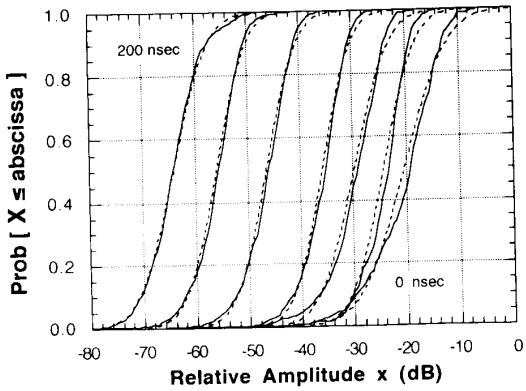


Fig. 7. Global distribution of signal amplitudes for Bldg 1, antenna separation of 5 m. Each set of curves from right to left represent distributions for excess delays of 0, 5, 25, 50, 100, 150, and 200 ns, respectively. Solid lines are experimental, dotted lines the theoretical lognormal fit distributions.

peak amplitude does not belong to the component of 0 excess delay [e.g., Fig. 2(b)]. As shown in Fig. 6, mean relative amplitudes decrease almost linearly with increasing excess delay until they reach an asymptote due to noise masking of signal peaks. Raw data, rather than binned data, were used to plot Fig. 6.

The distribution of individual multipath component amplitudes over global areas was also obtained. Global area data are those collected with one antenna separation (i.e., 1500 profiles). Empirical distributions were fit to theoretical lognormal, Rayleigh, Rice, Nakagami, and Suzuki (or mixed) distributions. These distributions are often mentioned in the literature in connection with signal amplitude fading (e.g., [25]). Parameters of the theoretical distributions were estimated from the empirical data. Since the amount of data is enormous, the experimental and theoretical distributions were calculated and compared for the amplitudes of multipath components occupying each one of 15 selected bins. A total of 120 global distributions (2 buildings × 4 antenna separations per building × 15 bins per antenna separation) were thus obtained.

Elaborate goodness-of-fit tests based on the Kolmogorov–Smirnov procedure [32] proved the supremacy of lognormal distribution in describing the amplitudes over global areas. Lognormal distribution passed the Kolmogorov–Smirnov test with 90% confidence for 87% of the cases tested.[4] Other theoretical distributions passed the test marginally for less than 11 cases (i.e., less than 10%).

Empirical and theoretical lognormal-fit distributions for Bldg 1, antenna separation of 5 meters, and for selected excess delays are reproduced in Fig. 7. Amplitudes are relative to the strongest component of all 1500 profiles at 5 m. Visual inspection of these figures show the excellent lognormal fit to the data. These curves represent (from left to right) distributions for excess delays of 0, 5, 25, 50, 100, 150, and 200 ns, respectively. The associated standard deviations are 6.6, 9.3, 4.9, 4.1, 4.6, and 4.9 dB, respectively. These are typical standard deviations observed for other global amplitude distributions of both buildings. In general, standard deviations for the amplitude of initial multipath components are higher than those of the latter ones. This is because there is greater variation among the initial paths of two different local areas, e.g., the impulse response function at one location may contain a strong LOS component at 0 excess delay while the other may have a severely attenuated component at the same delay.

Studying the literature shows no direct reference to the global statistics of path amplitudes. It has, however, been shown that the mean value of amplitudes at a fixed delay for data collected at different 1–2 m locations in several factory environments are lognormal [10]. Randomness of the local mean amplitudes at a fixed delay is due to the mid-scale variations of indoor channels described previously (Fig. 1).

*2) Local distributions:* Experimental distributions of single component amplitudes over local areas were also obtained. Local area data consists of all profiles collected at one 1.5 m location (i.e., 75 profiles). Since the number of samples for later portions of the excess delay axis are not sufficient, several adjacent bins were combined in order to increase the number of samples. This is justified since multipath components in these bins have similar statistics.

Empirical distributions for ten portions of the excess delay axis at each one of the 80 locations (2 buildings × 4 antenna separations × 20 locations per antenna separation) were obtained. Among the resulted 1600 cases considered, the lognormal distribution passed the Kolmogorov–Smirnov test with a 90% confidence level for 75% of cases. Rayleigh and Nakagami distributions (which are often mentioned in connection with amplitude fading over local areas) passed the test with the same confidence level for 12.5% and 36% of cases, respectively. Empirical and theoretical lognormal-fit distributions for a LOS location at Bldg 2 (antenna separation of 10 m) are shown in Fig. 8. Amplitudes are relative to the strongest component of all 1500 profiles at 10 m. The good lognormal fit observed in this figure is typical of what was observed for other cases at both buildings.

Standard deviations for local distributions are in the 3–5 dB range for most locations of both buildings. They are, in

[4]The Kolmogorov–Smirnov tests for both global and local amplitude distributions were carried out by H. Nikookar at Sharif University of Technology.

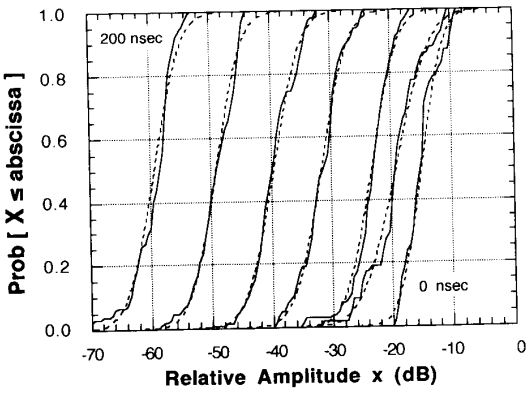


Fig. 8. Local distribution of signal amplitudes for a line-of-sight location at Bldg 2. Antenna separation is 10 m. Each set of curves from right to left represent distributions for excess delays of 0, 5, 25, 50, 100, 150, and 200 ns, respectively. Solid lines are experimental, dotted lines the theoretical lognormal fit distributions.

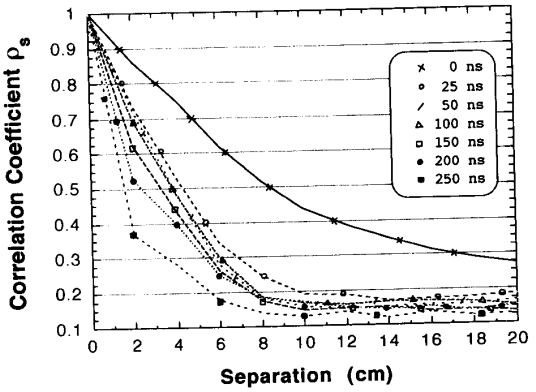


Fig. 9. Average spatial correlation coefficient on signal amplitudes $\rho_S$ for Bldg 1, all 6000 profiles combined. Curves from top to bottom represent excess delays of 0, 25, 50, 100, 150, 200, and 250 ns, respectively. Horizontal axis is sampling distances, vertical axis is $\rho_S$.

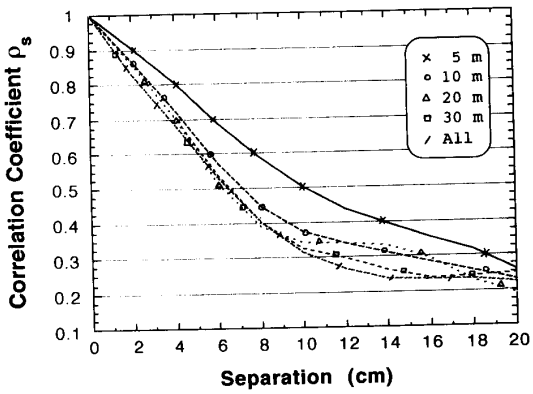


Fig. 10. Average spatial correlation coefficient $\rho_S$ for the direct path (0 excess delay) at Bldg 2. The curves from top to bottom represent antenna separations of 5, 10, 20, 30 m, and all 6000 profiles combined, respectively.

general, lower than those of the global distributions. This is expected since small-scale variations are less than mid-scale variations (Fig. 1).

Good lognormal fit to the local data is consistent with the results reported by another investigator using 20 samples per location [7], [10].

*3) Spatial correlations:* Impulse response estimates collected in the same "local" area are grossly similar since the channel's structure does not change appreciably over short distances. This can be observed from the adjacent profiles shown in Fig. 2.

Using the large data base of 12 000 profiles, the *average* spatial correlation coefficient of the amplitudes ($\rho_S$) was estimated as a function of both spatial displacement of the portable antenna and excess delay. The averages were taken over 20 locations that had the same antenna separation [in each building]. The binned data were used for this analysis.

A set of curves for $\rho_S$ versus displacement of the portable antenna in Bldg 1 are reproduced in Fig. 9. Each curve represents one excess delay. In these curves, $\rho_S$ is averaged over all locations and over all antenna separations. Similar results were obtained for Bldg 2 and for each antenna separation. Average spatial correlation coefficients for the direct path in Bldg 2, antenna separations of 5, 10, 20, and 30, and for all the 6000 profiles combined are reproduced in Fig. 10. An inspection of these figures and many more not reproduced shows that:

i) $\rho_S$ assumes its highest values for the direct path and consistently decreases with increasing the excess delay. This can be observed from curves in Fig. 9. This is reasonable since the direct path normally consists of a stable path, while later components undergo one or more reflections and hence are more random and less correlated.

ii) $\rho_S$ is insensitive to antenna separation, i.e., the same degree of correlation was observed for $d = 5$, 10, 20, and 30 m. This can be observed from curves in Fig. 10. An exception is the direct path (path with zero excess delay), where the 5 m data showed higher correlations. This is reasonable since the direct path is more likely to be a LOS path for the 5 m data, as compared to that measured with larger antenna separations. Greater stability of LOS signals are reflected in higher correlations for the 5 m data.

iii) $\rho_S$ for the direct path (0 excess delay) starts at about 0.9 for 2 cm separation and decreases to about 0.4 at 10 cm. Later multipath components have correlations between 0.4 and 0.8 at 2 cm separation and less than 0.2 at 10 cm. These are evident in Fig. 9.

*4) Delay correlations:* Amplitudes of adjacent multipath components of the same profile may be correlated since some of the scattering objects that produce them can be the same. This type of correlation has been observed in the mobile channel [24]. Analysis of the local data for both buildings, however, showed small correlation between the log amplitudes of adjacent multipath components. Furthermore, such correlations seem to be independent of antenna separation. The average correlation coefficient (average of 80 values obtained, one value for each local area) were estimated for each building. Average correlation coefficients between the first and second, second and third, and third and fourth paths were found to be 0.27, 0.23, and 0.21, respectively, for Bldg 1. The values for

TABLE III
MEAN ($\mu$) AND STANDARD DEVIATION ($\sigma$) FOR THE RMS DELAY SPREAD FOR BOTH BUILDINGS, ANTENNA SEPARATIONS OF 5, 10, 20, 30 m, AND $\alpha$ = 10, 20, AND 30 dB. VALUES ARE IN NANOSECONDS

| | Building 1 | | | | | | | | Building 2 | | | | | | | |
|---|---|---|---|---|---|---|---|---|---|---|---|---|---|---|---|---|
| | Antenna Separations (meters) | | | | | | | | Antenna Separations (meters) | | | | | | | |
| | 5 | | 10 | | 20 | | 30 | | 5 | | 10 | | 20 | | 30 | |
| $\alpha$ | $\mu$ | $\sigma$ | $\mu$ | $\sigma$ | $\mu$ | $\sigma$ | $\mu$ | $\sigma$ | $\mu$ | $\sigma$ | $\mu$ | $\sigma$ | $\mu$ | $\sigma$ | $\mu$ | $\sigma$ |
| 10 dB | 8.4 | 4.5 | 11.4 | 5.3 | 17.0 | 7.8 | 19.9 | 10.7 | 9.7 | 4.5 | 12.6 | 5.3 | 14.0 | 6.2 | 16.3 | 7.0 |
| 20 dB | 14.3 | 4.2 | 17.9 | 4.7 | 25.0 | 9.0 | 30.9 | 11.3 | 15.3 | 4.1 | 18.4 | 5.0 | 21.1 | 5.7 | 23.9 | 6.5 |
| 30 dB | 16.9 | 4.2 | 20.7 | 4.3 | 28.2 | 8.7 | 35.5 | 11.0 | 17.5 | 3.9 | 20.7 | 4.6 | 23.7 | 5.2 | 26.6 | 6.0 |

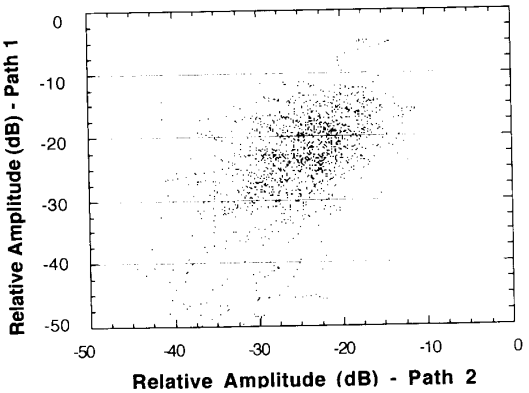


Fig. 11. Scatter diagram of log amplitudes (first versus second path) for Bldg 1. The 1500 points represent data for one global area (antenna separation of 10 m).

Bldg 2 were 0.29, 0.18, and 0.18, respectively. The fact that, in general, delay correlations decrease with increasing excess delay is intuitively clear since later multipath components go through multiple reflections more often as compared to components with shorter delays (since, *on the average,* attenuation is higher for longer delayed paths—Fig. 6). Multiple reflections result in more randomness and smaller correlation. It should also be mentioned that although the binned data were used for estimating correlation coefficients, adjacent components are not necessarily components in adjacent bins. Therefore, differential delays are variable (multiples of 5 ns), which may be another reason for observing small correlations.

A typical global scatter diagram for the log amplitudes of initial paths are reproduced in Fig. 11. In this figure, all 1500 profiles at Bldg 1 with antenna separation of 10 m are included.

### D. Analysis of RMS Delay Spread

A single-number representation of an impulse response function is the rms delay spread $\tau_{\text{rms}}$ defined as

$$\tau_{\text{rms}} = \left\{ \left[ \sum_k (t_k - \tau_m - t_A)^2 a_k^2 \right] \Big/ \sum_k a_k^2 \right\}^{\frac{1}{2}} \quad (4)$$

where $t_A$ is the arrival time of the first path in a profile and $\tau_m$ is the mean excess delay defined as

$$\tau_m = \left[ \sum_k (t_k - t_A) a_k^2 \right] \Big/ \left[ \sum_k a_k^2 \right]. \quad (5)$$

$\tau_{\text{rms}}$ is the square root of the second central moment of a power delay profile $|h(t)|^2$. $\tau_{\text{rms}}$ is a good measure of multipath spread; it gives an indication of the potential for intersymbol interference.

The rms delay spread $\tau_{\text{rms}}$ was calculated for each one of the 12 000 impulse response estimates. The raw data (rather than the binned data) were used for the calculations. Subsequently, $\tau_{\text{rms}}$ was analyzed over both local and global areas. Mean and standard deviation of $\tau_{\text{rms}}$ values for both buildings and different antenna separations are listed in Table III. $\tau_{\text{rms}}$ values are typically between 10 and 50 ns, with a mean value in the 20–30 ns range. These values are consistent with the median value of 26 ns reported for a university campus building [19], and 25 ns for a medium-size office building [21]. A standard deviation of 8 ns has been reported in [19], which is also consistent with the entries of Table III.

$\tau_{\text{rms}}$ increases with increasing $\alpha$ (range in dB relative to the strongest path of a profile) since more multipath components are included for larger $\alpha$ (Table III).

Delay spread values have a normal distribution over global areas (i.e., over all locations with the same antenna separation—a total of 1500 profiles). This can be observed from the empirical and theoretical normal-fit distributions for Bldg 2 reproduced in Fig. 12. The good normal fit is preserved when all 6000 profiles for one building are combined.

The average delay spread increases when the transmitter/receiver antenna separation increases from 5 to 30 m. This is evident from Table III and Fig. 12. The standard deviation of $\tau_{\text{rms}}$ also increases with increased antenna separation (Table III); the explanation is that the propagation path becomes more nonuniform for larger separations.

The mean rms delay spread for each location was obtained by averaging 75 individual $\tau_{\text{rms}}$ values. The average path loss, in dB, for each location was also obtained by subtracting the received power (sum of the power of individual multipath

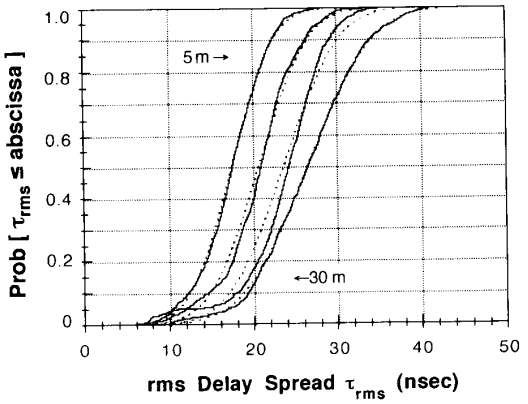


Fig. 12. Distribution functions of $\tau_{\rm rms}$ for Bldg 2. Each set of curves from left to right represent antenna separation of 5, 10, 20, and 30 m, respectively. Solid lines are the empirical distributions and dotted lines the normal-fit distributions.

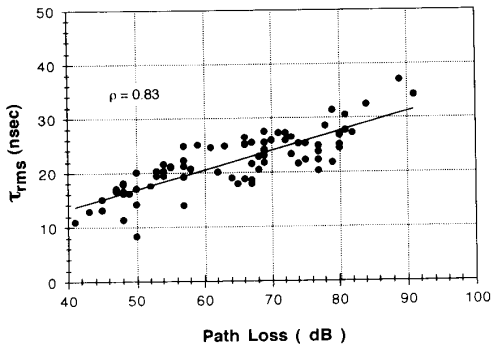


Fig. 13. Mean rms delay spread (in ns) for each location versus average path loss (in dB) for that location. Each point represents the averages for one location of Bldg 2.

components) from the transmitted power for each impulse response estimate and averaging the 75 resulting values. The mean $\tau_{\rm rms}$ for each location shows a great linear dependence with the average path loss for that location, as evident in the scatter diagram of Fig. 13. The increase in $\tau_{\rm rms}$ with range and path loss is probably due to the fact that the powers of long delayed components, relative to those of the earliest received signals, are greater in such cases than they are in cases where the "direct" path loss is lower.

A full report of the results of this aspect of the analysis can be found in [2], [5].

## V. Summary and Conclusion

Statistical analysis of the indoor radio propagation data collected at two dissimilar buildings was reported. The data base included 12 000 estimates of the channel's impulse response (75 samples per small locations × 20 locations per antenna separation × 4 antenna separations of 5, 10, 20, and 30 m per building). Impulse response estimates were obtained by inverse Fourier transforming the channel's equivalent transfer functions. Using the resulting large multipath propagation data base, small-scale, mid-scale, and large-scale variations of the channel were investigated. Extensive sets of plots and tables for both buildings were obtained, a small number of which were reproduced in this paper.

The number of multipath components in each profile $N$ was found to be a Gaussian-like distributed random variable with a mean value that increases with increased antenna separation. When all components of a profile with amplitudes within 30 dB of the peak amplitude were included, the mean of $N$ increased from 13 to 24 for Bldg 1 and from 13 to 19 for Bldg 2 as the antenna separation increased from 5 to 30 m. Standard deviations were between 3 and 7, also increasing with distance.

A Poisson fit to the arrival times of multipath components proved to be unsatisfactory. A modified Poisson process (the $\Delta$-$K$ model) provided good fits to the data for both buildings and all antenna separations. Most $K$ values were in the 0.5–0.8 range, indicating that paths are often less clustered than what a standard Poisson process dictates.

The distribution of the amplitude of individual multipath components was obtained for both global data (1500 profiles representing one antenna separation) and local data (75 profiles representing one location). The lognormal distribution passed the Kolmogorov–Smirnov test of goodness of fit with a 90% confidence level for majority of cases tested (87% for global data and 75% for local data). For global data, standard deviations were in the 4–10 dB range, decreasing with increased excess delay. Local data showed smaller standard deviations of 3–5 dB. Mean amplitudes of multipath components (in dB relative to the peak amplitude of each profile) decrease almost linearly with increased excess delay for both local and global data, although only the results for global data were presented.

Correlation on log amplitudes for impulse response estimates of spatially adjacent points were investigated. The average correlation coefficient $\rho_S$ is between 0.7 and 0.9 for the portable antenna displacement of 2 cm, but it drops fairly rapidly for larger displacements. $\rho_S$ is about the same for all antenna separations, with the exception of the 5 m data (which showed higher correlations). The values of $\rho_S$ are greater for the initial paths than for later paths.

Amplitude of adjacent multipath components of the same profile showed little correlation for both buildings. Typical correlation coefficients are between 0.2 and 0.3.

The rms delay spread $\tau_{\rm rms}$ showed a clear dependence with antenna separation. When multipath components within 30 dB of the peak amplitude in each profile are combined, $\tau_{\rm rms}$ increases from 16.9 to 35.5 for Bldg 1 and from 17.5 to 26.6 for Bldg 2 as antenna separation increases from 5 to 30 m. The standard deviations also increase with increased antenna separation. Average $\tau_{\rm rms}$ for each location shows a great linear dependence with average path loss for that location.

The results reported in this paper can be used in the performance analysis and design of indoor radio communication systems, either directly or through an elaborate simulation model based on the reported statistical characterization. One scenario for the development of a computer simulation model that generates a consistent set of spatially adjacent impulse response estimates is as follows.

For a given transmitter/receiver antenna separation, the sequence of arrival times corresponding to impulse response estimates for one location are generated according to the discrete-time $\Delta$-$K$ model. $\Delta$ is fixed at 5 ns (width of one bin, equal to the resolution of measurements), $K$ is obtained from Table II, and the underlying probabilities of having multipath components in different bins are computed from $K$ and the empirical probability of occupancies (Fig. 4) using the appropriate equations [25], [26]. Since local amplitude distributions are lognormal (Fig. 8) and delay correlations are negligible, for the first profile in a location relative amplitudes (in dB) are generated according to independent normal distributions with a mean that decreases with increasing excess delay (Fig. 6). For subsequent profiles of the same location, relative amplitudes in dB are generated according to bivariate normal distributions, taking spatial correlations into account (Figs. 9 and 10). When impulse response estimates are combined, their statistics should match the global statistics (such as the global distributions of the number of multipath components given in Table I and Fig. 3, and the global amplitude distributions of Fig. 7). Furthermore, the simulation model should be capable of reproducing statistics of the rms delay spread of empirical data (Table III, Figs. 12 and 13). The impulse response estimates corresponding to transmitter/receiver antenna separations of 5, 10, 20, and 30 meters are thus generated. For other antenna separations, simulation may be based on parameters calculated through linear interpretation or extrapolation between the results obtained in this project.

Although there are many technical details involved in generating an elaborate channel simulator [26], our sketch shows the utility of the results reported in this paper. Most of these results (e.g., the amplitude distributions and statistics of $N$ and $\tau_{\text{rms}}$) can also be used directly in performance evaluation of indoor communication systems.

Analysis of the extensive multipath data base established throughout the measurement campaign is in progress. The goal is to obtain smaller details about the channel, refine the statistical model reported in this paper, and eventually simulate it on a digital computer.

## ACKNOWLEDGMENT

A heavy debt of gratitude is due to D. Tholl of NovAtel (currently with TRLabs), without whose dedicated efforts this project would not have been completed. Special thanks are due to D. Lee and D. Ehman of NovAtel for software assistance in processing the data. The author acknowledges, with great pleasure, his association with Dr. R. J. C. Bultitude of CRC in Ottawa during this period. Last, but not least, the support and encouragement of NovAtel's management (especially J. Chinnick, Vice President of Research and Development) throughout this project is gratefully acknowledged.

## REFERENCES

[1] H. Hashemi, "The indoor radio propagation channel," to appear in *Proc. IEEE*, vol. 81, no. 7, July 1993.

[2] H. Hashemi and D. Tholl, "Analysis of the rms delay spread of indoor radio propagation channels," in *Proc. IEEE Int. Conf. Commun.*, Chicago, IL, June 1992, pp. 875–881.

[3] H. Hashemi, D. Tholl, and G. Morrison, "Statistical modeling of the indoor radio propagation channel—Part I," in *Proc. IEEE Vehic. Technol. Conf.*, Denver, CO, May 1992, pp. 338–342.

[4] H. Hashemi, D. Lee, and D. Ehman, "Statistical modeling of the indoor radio propagation channel—Part II," in *Proc. IEEE Vehic. Technol. Conf.*, Denver, CO, May 1992, pp. 839–843.

[5] H. Hashemi and D. Tholl, "Statistical modeling and simulation of the RMS delay spread of indoor radio propagation channels," *IEEE Trans. Vehic. Technol.*, 1993.

[6] D. Molkdar, "Review on radio propagation into and within buildings," *IEE Proc.*, pt. H, vol. 138, no. 1, pp. 61–73, Feb. 1991.

[7] T. S. Rappaport and C. D. McGillem, "UHF fading in factories," *IEEE J. Select. Areas Commun.*, vol. 7, no. 1, pp. 40–48, Jan. 1989.

[8] T. S. Rappaport, "Indoor radio communications for factories of the future," *IEEE Commun. Mag.*, pp. 15–24, May 1989.

[9] T. S. Rappaport, "Characterization of UHF multipath radio channels in factory buildings," *IEEE Trans. Anten. and Propagat.*, vol. 37, no. 8, pp. 1058–1069, Aug. 1989.

[10] T. S. Rappaport, S. Y. Seidel, and K. Takamizawa, "Statistical channel impulse response models for factory and open plan building radio communication system design," *IEEE Trans. Commun.*, vol. 39, no. 5, pp. 794–807, May 1991.

[11] D. M. J. Devasirvatham, "Time delay spread and signal level measurements of 850 MHz radio waves in building environments," *IEEE Trans. Anten. and Propagat.*, vol. AP-34, no. 11, pp. 1300–1305, Nov. 1986.

[12] D. M. J. Devasirvatham, "A comparison of time delay spread and signal level measurements within two dissimilar office buildings," *IEEE Trans. Anten. and Propagat.*, vol. AP-35, no. 3, pp. 319–324, Mar. 1987.

[13] D. M. J. Devasirvatham, "Multiple time delay jitter measured at 850 MHz in the portable radio environment," *IEEE J. Select. Areas Commun.*, vol. SAC-5, no. 5, pp. 855–861, June 1987.

[14] D. M. J. Devasirvatham, "Multiple time delay spread in the digital portable radio environment," *IEEE Commun. Mag.*, vol. 25, no. 6, pp. 13–21, June 1987.

[15] K. Pahlavan, R. Ganesh, and T. Hotaling, "Multipath propagation measurements on manufacturing floors at 910 MHz," *Electron. Lett.*, vol. 25, no. 3, pp. 225–227, Feb. 1989.

[16] R. Ganesh and K. Pahlavan, "Statistical modeling and computer simulation of the indoor radio channel," *IEE Proc. Part I: Commun., Speech and Vision*, vol. 138, no. 3, pp. 153–161, June 1991.

[17] S. Howard and K. Pahlavan, "Measurement and analysis of the indoor radio channel in the frequency domain," *IEEE Trans. Instrument. and Measure.*, vol. IM-39, pp. 751–755, Oct. 1990.

[18] R. J. C. Bultitude, "Measurement, characterization and modeling of indoor 800/900 MHz radio channels for digital communications," *IEEE Commun. Mag.*, vol. 25, no. 6, pp. 5–12, June 1987.

[19] R. J. C. Bultitude, S. A. Mahmoud, and W. A. Sullivan, "A comparison of indoor radio propagation characteristics at 910 MHz and 1.75 GHz," *IEEE J. Select. Areas Commun.*, vol. 7, no. 1, pp. 20–30, Jan. 1989.

[20] R. J. C. Bultitude, "Measurements of wideband propagation characteristics for indoor radio with predictions for digital system performance," in *Proc. Wireless'90 Conf.*, Calgary, Alberta, Canada, July 1990.

[21] A. A. M. Saleh and R. A. Valenzuela, "A statistical model for indoor multipath propagation," *IEEE J. Select. Areas Commun.*, vol. 5, no. 2, pp. 128–137, Feb. 1987.

[22] H. Zaghloul, G. Morrison, D. Tholl, R. J. Davies, and S. Kazeminejad, "Frequency response measurements of the indoor channel," in *Proc. ANTEM'90 Conf.*, Winnipeg, Manitoba, Aug. 1990, pp. 267–272.

[23] G. L. Turin, "Communication through noisy, random-multipath channels," *1956 IRE Conven. Rec.*, pt. 4, pp. 154–166.

[24] G. L. Turin *et al.*, "A statistical model of urban multipath propagation," *IEEE Trans. Vehic. Technol.*, vol. VT-21, pp. 1–9, Feb. 1972.

[25] H. Suzuki, "A statistical model for urban radio propagation," *IEEE Trans. Commun.*, vol. COM-25, pp. 673–680, July 1977.

[26] H. Hashemi, "Simulation of the urban radio propagation channel," *IEEE Trans. Vehic. Technol.*, vol. VT-28, pp. 213–224, Aug. 1979.

[27] G. L. Turin, "Introduction to spread-spectrum antimultipath techniques and their application to urban digital radio," *Proc. IEEE*, vol. 68, no. 3, pp. 328–353, Mar. 1980.

[28] W. H. Lam and R. Steele, "The error performance of CD900-like cellular mobile radio systems," *IEEE Trans. Vehic. Technol.*, vol. 40, no. 4, pp. 671–685, Nov. 1991.

[29] F. J. Harris, "On the use of windows for harmonic analysis with the discrete Fourier transform," *Proc. IEEE*, vol. 66, no. 1, Jan. 1978.

[30] W. H. Press *et al.*, *Numerical Recipes in C*. Cambridge, MA: Cambridge Univ. Press, 1988.

[31] D. Tholl, "Frequency response measurements in two buildings," NovAtel Commun. Ltd. int. rep., Sept. 1991.

[32] R. V. Hogg and E. A. Tanis, *Probability and Statistical Inference.* New York: Macmillan, 1977, pp. 280–285.

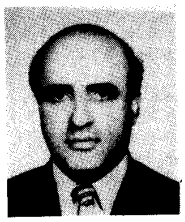

**Homayoun Hashemi** (M'89) was born in Teheran, Iran. He received the B.S.E.E. degree from the University of Texas, Austin, in 1972, the M.S. and Ph.D. degrees in electrical engineering and computer sciences from the University of California, Berkeley, in 1974 and 1977, respectively, and the M.A. degree in statistics from the University of California at Berkeley.

In the summer of 1977, he served as a Consulting Engineer at Stanford Research Institute, Menlo Park, CA. From 1977 to 1979, he was a Member of Technical Staff at Bell Telephone Laboratories, Holmdel, NJ, where he was involved in system design for high-capacity mobile telephone systems. Since 1979, he has been a Faculty Member at the Electrical Engineering Department of Sharif University of Technology in Teheran, Iran, where he is currently an Associate Professor. He was on sabbatical leave at NovAtel Communications Ltd. in Calgary, Alberta, Canada during the 1990–1991 academic year, where he worked on various projects related to mobile and personal communications. He spent the summer of 1992 at the Electrical Engineering Department of the University of Ottawa, where he was involved in propagation modeling of optics for indoor wireless communications. In the summer of 1993, he was a Visiting Researcher at TRLabs in Calgary, where he worked on wireless indoor radio communications. He has done research on different aspects of wireless communications, including general system architecture, channel assignment, propagation modeling, performance analysis, and capacity evaluations for digital cellular, microcellular, and indoor wireless communication systems. His channel simulator package SURP has been used internationally in the design of digital cellular mobile radio communication systems. He has also served as a consultant to the Telecommunication Company of Iran and the Iranian Telecommunication Research Center, and has contributed to different telecommunication expansion projects in Iran.